IMPLICATIONS OF JITTER ON HIGH SPEED SERIAL INTERFACE STANDARDS, SIMULATION, AND DESIGN

MSEE PROJECT

JOHN BENNETT

DR. UN-KU MOON

WINTER 2004

TABLE OF CONTENTS

IMPLICATIONS OF JITTER ON HIGH SPEED SERIAL INTERFACE STANDARDS, SIMULATION, AND DESIGN

1. INTRODUCTION

As technology sizes decrease, pin geometry is not keeping pace. This has led to widespread use of high speed serial interfaces to maximize use of silicon real estate. The signals in these systems are corrupted by large amounts of distortion and interference. As data rates increase, accurate characterization of distortion and its impact becomes even more important. Systems engineers create signaling budgets by analyzing physical imperfections and describing their impacts on the system.

One large obstacle in receiving the signal is jitter accumulated during the transmission and link. Throughout this paper, jitter refers to a variation in time from the ideal. This is a major hurdle in design. The receiver must know when it can accurately detect the signal. As jitter increases, that window of opportunity decreases.

Jitter has various sources. Electrical transmission channels have a low pass filtering effect, adding intersymbol interference (ISI) and frequency dependent attenuation. Optical channel media does not add notable ISI, but it does add random phase noise. Propagation through the channel exposes the signal to interferers via coupling and other sources of distortion, like reflections. The transmitter adds jitter resulting from random circuit-level effects as well as a finite bandwidth. The receiver also distorts the signal through additional filtering, and random noise.

At the composition of this paper, the edge-of-the-envelope in manufacturable serializer/deserializer (SERDES) performance is 40 Gb/sec, 10 Gb/sec for CMOS. This speed is phenomenal, accurately transmitting and receiving signals with bit periods of <25ps. Increases in transmission speed cause the unit interval (UI), or bit period, to decrease. Thus, a fixed amount of jitter has a much larger impact in high-rate systems than low-rate counterparts.

Effects from low frequency interferers can be removed. A clock recovery circuit, generally a phase locked loop, has the ability to track out these signals. The circuitry tracks variations in the transition point versus time and shifts the system's clock to match these variations.

The undesirable high-frequency signals are not removed with that circuit, but the return loss at the receiver helps to reject them. Additional high frequency jitter is removed by the PLL attached to the reference crystal. PLLs have a low pass frequency response. If equalization is performed at the receiver, out of band signals can be attenuated further.

Jitter and other interferers are also present in the band between tracked and filtered signals. This is also the frequency band where the data resides. Therefore, the system must be able to tolerate these distortions.

Interfaces for commercial systems are specified in both implementation agreements and standards. These ensure intersystem compatibility between products from multiple vendors. For SERDES, the various standards (from OIF, InfiniBand, Fibre Channel, IEEE, etc.) will be referred to herein simply as "Standards." The physical layer sections within Standards describe electrical performance requirements for the transmitter and the receiver.

Jitter requirements for the transmitter specify maximum levels of jitter on the emitted data signal. Receiver requirements on the other hand, describe jitter the receiver must tolerate on the received signal while satisfying a minimum bit error rate (BER).

The specifications for receive jitter have to be translated to the system jitter budget. This work will show three aspects of jitter in systems. The first is to illustrate impacts the jitter proportions (random and deterministic) have on the expected signal. Second, the spectrum of random jitter is important in determining its effects and the required bandwidth for the receiver. Finally, the specified random jitter can be transformed into a deterministic jitter specification used in the jitter budget and simulation.

2. JITTER

Jitter refers to the variation in time of an event from its ideal location. In a non-return to zero (NRZ) encoding scheme, the transitions occur at well defined points in time, integer multiples of the symbol period. The jitter on this type of signal is consequently easy to measure. Multiple sources cause these variations, and not all effect the signal in the same way.

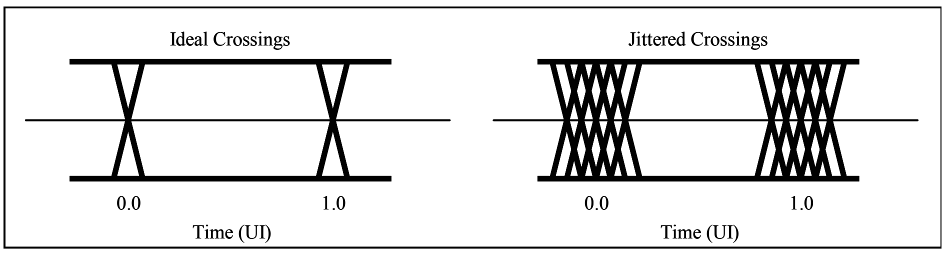

Figure 1: (a) Ideal Crossings (b) Jittered Crossings

Various methods are used to describe the jitter components. This paper uses the statistical classifications of deterministic (DJ) and random jitter (RJ). The difference between the two is the deterministic jitter is bounded, while the random is not. One symbol period is referred to as a unit interval (UI), shown in Figure 1 (a). Jitter skews the crossing points, varying the transition locations in time (Figure 1 (b)).

Jitter reduces the time period where a valid sample can be taken, possibly so much that the receiver cannot properly detect the signal. The components of jitter are described in the following sections.

2.1. DETERMINISTIC JITTER

The bounded nature of DJ allows for a specific bound on jitter rather than the probabilistic description of RJ. Multiple sources account for the DJ in the system. They are described below.

2.1.1. Data Dependent Jitter

Data dependent jitter (DDJ) is directly proportional to the transmitted symbols. The primary form is intersymbol interference (ISI). This results directly from symbols passing through a bandwidth limiting channel. The impact is proportional to the spectral response of the channel and its relationship to the bandwidth of the data pattern transmitted. For example, a high bandwidth pattern passing through a low bandwidth channel will have a considerable amount of interference at the output.

The channel acts much like a linear filter and is easily modeled. One such technique uses a pole-zero modeling for the transmission line frequency response to create a filter. This model is developed for the longest channel of interest and the poles and zeros are scaled appropriately for shorter channel lengths. (HUSS, HUSS & BENNETT)

There are only a finite number of bit sequences corresponding to the memory of a channel (the length of its impulse response), which yields nicely for modeling. The ISI crossing points will occur at finite instances, each having their own probability. The use of multiple delta functions models this nicely. Standards actually take a slightly more simplified approach, called the “dual dirac-delta model.” (MJSQ).

The foundation of the dual-dirac delta model is that the ISI will move crossings one direction or the other, resulting from the adjacent symbols. For data bandwidths less than 3GHz, this is a safe assumption. However, as backplane speeds increase we find it to be increasingly poor. Samples can be influenced by ten or more adjacent symbols. Current standards (11G+ Interfaces) have no eye opening at the receiver, so equalization becomes mandatory and compliant channel specification is very difficult.

2.1.2. Duty Cycle Distortion

Duty Cycle Distortion (DCD) refers to the time difference between a '1' and a '0'. The common source of this error is shifting bias points and varying rise and fall times of system components (HFAN-4.0.3). For example, a slight DC component added to a sinusoid causes the time spent above and below the origin to be unequal. This should not be confused with ISI and can only be measured on a clock-like signal, ('…101010…') to remove the other effects. The interfaces are differential, so no frequency modulation results.

2.1.3. Sinusoidal Jitter

Sinusoidal jitter (SJ) is a type of deterministic jitter where the time displacement of the signal follows a sinusoidal pattern. This type of jitter is rarely seen in practice (HFAN-4.0.3) but is widely used in compliance testing to serve as a margin (MJSQ, CEI, 802.3AP). The worst cases for pulse shifting or pulse-width modulation can be simulated by changing both the frequency and amplitude of the SJ.

2.1.4. Uncorrelated Jitter

Physical interfaces and signal paths lead to additional signal degradations. For instance, EMI from either traces or pins coupling can lead to DCD or an additional uncorrelated signal being received. Interferers can also couple onto the PLL's reference signal. Power supply noise, internal switching noise, crosstalk, signal reflections, optical laser source noise, etc., are included in this category. These types of interferers can be modeled by a uniform random jitter that is bounded, following a white amplitude distribution.

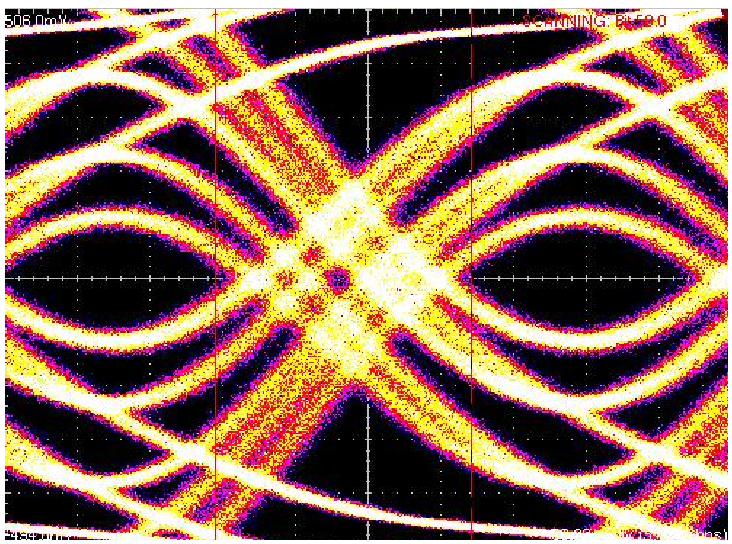

Figure 2: Impact of DJ

2.1.5. Effects

As illustrated in Figure 2, DJ produces a bounded shifting of the transitions. The various components have unique characteristics. DDJ and DCD are quite similar, resulting in discrete transition points. Both SJ and uncorrelated jitter spread the discrete crossings, similar to RJ. One interesting point not so obvious from the eye diagrams is that edge translation is the primary impact of DJ. ISI is the main source, which is similar to a linear filtering. While the symbol width changes, the frequencies are reduced, so a single-ended frequency modulation takes place, when viewed from the crossing point, but not a phase modulation of the differential signals.

2.2. RANDOM JITTER

2.2.1. Sources

Random jitter is caused by a variety of sources in the transmitter, as well as thermal noise in the channel. Origins are reference crystal phase noise, shot noise, flicker noise, and thermal noise.

Shot noise is process dependent, varying proportional to current fluctuations about the average value. Flicker noise is a $1/f$ noise, and is due to random capturing and emittance of electrons from oxide interfaces. Thermal noise primarily effects systems with a low SNR, and is due to scattering of electrons in the lattice. The scattering increases with lattice vibrations, and is due to temperature increases. At low temperatures, scattering, and hence RJ, will still be present due to lattice imperfections. (JITTER FUNDAMENTALS)

2.2.2. Characterization

RJ is modeled by a Gaussian distribution for two reasons: the jitter is not bounded; and, it is a random value whose amplitude distribution has a Gaussian characteristic (Figure 3). Gaussian distributions are described by their mean and standard deviation, or

RMS value. A bound can be set on a Gaussian's amplitude by including the probability of occurrence. This allows the RMS descriptor to be converted to a p-p value. For example, ($100-10^{-2}$) = 99.99% of the time (BER = 10^{-4}) a Gaussian with $\sigma = 1$ will have a magnitude less than 7.4380. This conversion is helpful for relating to DJ and for easily visualizing the effects on an eye diagram. Additional error rates are converted to p-p values for a Gaussian with $\sigma = 1$ in Table 1. These apply to a data signal that has an edge density of one. Lower edge densities (i.e. 0.5 for a random signal) scale this conversion to a lower peak-to-peak level since the jitter only effects transitions.

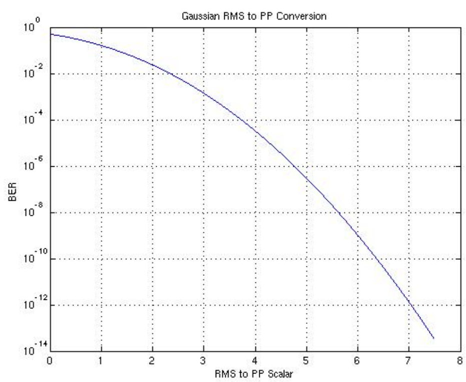

Probability	P-P
10^{-4}	7.4380
10^{-6}	9.5069
10^{-8}	11.224
10^{-10}	12.723
10^{-12}	14.069
10^{-14}	15.301

Table 1: Relationship between Gaussian peak-to-peak value and probability

2.2.3. Effects

The impact of RJ on the eye diagram is fairly straight forward. The RMS value should be converted to a peak-to-peak value at the error rate of interest. The resultant value is the amount the eye will be closed for the given error rate. However, RJ has a much more interesting and less obvious impact on the signal.

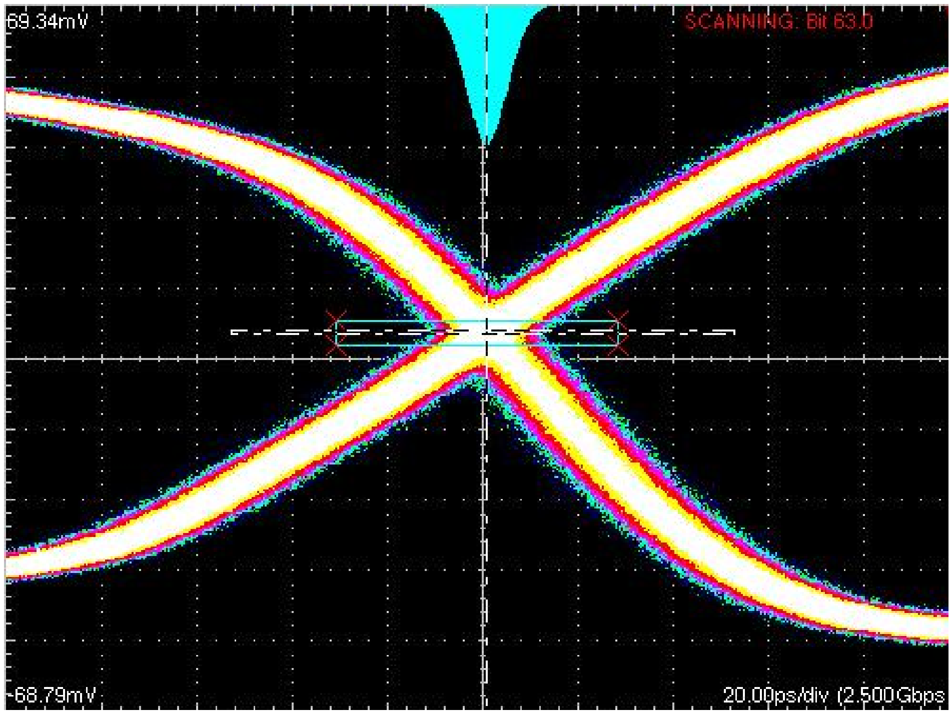

Figure 3: Gaussian Jitter Distribution

The time domain signal can look much different then expected from the eye diagram. If the jitter is low frequency, it will slowly move each edge of the eye, but move them together, shifting the symbol. The received symbols will have a very similar and low frequency relative to 1/(2*eye_width), even though the eye is at minimum width. However, a high frequency phase modulation can shift the edges in independent directions. This will produce a signal containing symbols of various periods, or frequencies, even though the eye shows the same closure.

The only method to increase a signal's bandwidth is by modulation. RJ acts like a phase-modulation on the data signal. Hence, the spectrum of the jitter has a large impact on the result, which translates into frequency changes of the data signal. This will be converted to a numerical relationship shortly. Figure 4 illustrates this concept. The red/dashed lines represent the highest frequency, yet their transition spacing is much greater than that allowed by the eye. You can also see that any additional attenuation on those highest frequency signals will cause them to violate the minimum eye height.

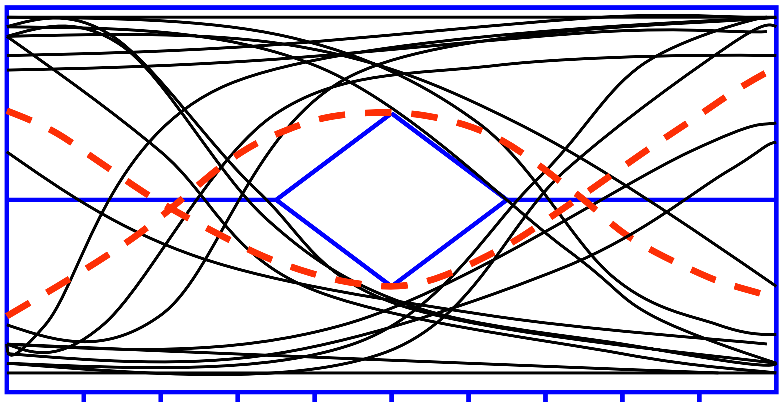

Figure 4: Modulation vs. Translation

The required bandwidth of the receiver is directly related to the highest frequency it must receive. For design, a quantitative relation between RJ and the maximum frequency will be very useful.

The relationship between RJ at sequential edges is determined by the spectrum of the jitter. If the spectrum is white and has a much wider bandwidth than that of the symbol rate, jitter present at subsequent edges is completely uncorrelated. On the other hand, bandwidth constraints (whether by specification or physical reality) on this jitter can force sequential transitions to be dependent on one or more previous values.

3. INFLUENCE OF SPECTRAL CHARACTERISTICS

Spectral influences from RJ were touched upon in the previous section. Prior to continuing that discussion, some probability theory should be presented.

3.1. JOINT DENSITY FUNCTION

The investigation performed here requires a description for the relationship between two samples. Consider one sample at time t_1 and another Δt later. The existence of correlation between the samples means the first sample influences the second. If the distribution is well described, this influence can be directly calculated.

RJ is described by a Gaussian distribution. Because the operation $x(t_2)-x(t_1)$ is linear, the result will also follow a Gaussian distribution (PAPOULIS & PILLAI). The probability density function (PDF) for a single Gaussian variable is described by:

$$f(x) = \frac{1}{\sqrt{2\pi\sigma^2}} \mathrm{e}^{\frac{-(x-\mu)^2}{2\sigma^2}} \tag{1}$$

The variance of the signal is needed for this calculation, and is given by:

$$\sigma = \mathrm{E}\{X^2\} - \mu^2 \qquad \text{(Variance)} \tag{2}$$

where μ represents the mean, and E{} is the expected value.

Two samples, x and y, are taken from this sequence at times t_1 and t_2, respectively. Correlation between the two sample points has two effects on the distribution of the second sample. First, the mean is offset by the correlation between the samples, scaled by the first's value. The other is the correlation scales the variance of the second sample's distribution. When correlation is present, the likelihood of occurrence for similar values is greater than that of dissimilar ones. Reduced variance quantifies this effect. The most likely location of the second sample centers near the expected value of the first. The distribution around this point is determined mathematically and results are available in various texts (STARK & WOODS).

$$f_{Y|X}(y|x) = \frac{1}{\sqrt{2\pi\left(1-\rho^2\right)}} \mathrm{e}^{\frac{-(y-\rho x)^2}{2\left(1-\rho^2\right)}} \tag{3}$$

The likelihood of the first variable having a particular value, *x*, is calculated from the PDF. The joint density is extended from this individual PDF. Even though the joint variables are subsequent samples out of one sequence with a Gaussian distribution, they will be treated as two separate distributions. The dependence is accounted for by the correlation coefficient used to describe the similarities of these variables, and calculated from the correlation between the two samples, scaled by the root product of their autocorrelations.

$$\rho = \frac{\mathrm{C}(t_1,t_2)}{\sqrt{\mathrm{C}(t_1,t_1)\mathrm{C}(t_2,t_2)}} \quad \text{(Correlation Coefficient)} \tag{4}$$

Writing the joint distribution in matrix form results in

$$f_x(x) = \frac{1}{2\pi\left[\det(\mathbf{K})\right]^{\frac{1}{2}}} \mathrm{e}^{\frac{-1}{2}(\mathbf{x}-\boldsymbol{\mu})^T \mathbf{K}^{-1}(\mathbf{x}-\boldsymbol{\mu})} \tag{5}$$

where,

$$\mathbf{K} = \begin{bmatrix} \sigma_x{}^2 & 0 \\ 0 & \sigma_y{}^2 \end{bmatrix} = \begin{bmatrix} \sigma_x{}^2 & 0 \\ 0 & \sigma_x{}^2\left(1-\rho^2\right) \end{bmatrix}$$

$$\det(\mathbf{K}) = \prod_{i=1}^{n} \sigma_i{}^2 = \sigma_x{}^4\left(1-\rho^2\right) \tag{6}$$

$$\mathbf{x} = \begin{bmatrix} x \\ y \end{bmatrix} \quad \mu = \begin{bmatrix} \mu_x \\ \mu_y + \rho x \end{bmatrix} = \begin{bmatrix} 0 \\ \rho x \end{bmatrix}$$

which expands to:

$$\begin{aligned} f_x(x) &= \frac{1}{2\pi\left[\sigma_x{}^4\left(1-\rho^2\right)\right]^{1/2}} \mathrm{e}^{-\frac{1}{2}\left(\begin{bmatrix} x \\ y-\rho x \end{bmatrix}^T \begin{bmatrix} \sigma_x{}^2 & 0 \\ 0 & \sigma_x{}^2\left(1-\rho^2\right) \end{bmatrix} \begin{bmatrix} x \\ y-\rho x \end{bmatrix}\right)} \\ &= \frac{1}{2\pi\sigma_x{}^2\sqrt{1-\rho^2}} \mathrm{e}^{\frac{-1}{2}\left(\frac{x^2}{\sigma_x{}^2}+\frac{(y-\rho x)^2}{\sigma_x{}^2\left(1-\rho^2\right)}\right)} \end{aligned} \tag{7}$$

and leads to the accepted Gaussian joint probability:

$$\begin{gathered} f_{xy}(x,y) = \frac{1}{2\pi\sigma^2\sqrt{1-\rho^2}} \mathrm{e}^{\frac{-1}{2\sigma^2\left(1-\rho^2\right)}\left(x^2+y^2-2\rho xy\right)} \\ x = x(t_1) - \mu \quad y = x(t_2) - \mu \end{gathered} \tag{8}$$

These results can be validated for intuitive test cases. First case: the joint probability of two independent processes is their individual probabilities multiplied together. Substituting $\rho=0$ results in exactly that, the product of two Gaussian PDFs. The other extreme is complete correlation ($\rho = 1$), and results in $f_{xy}(x,y)$ proportional to $\delta(y-x)$. For this final case, knowledge of the first sample enables the determination of the second with complete certainty. **(STARK & WOODS)**

The results from this function are best visualized with either a 3-dimensional or a contour plot. An example contour plot is shown in Figure 5. Two Gaussian joint probabilities are plotted here with correlations of 0.2339 and 0, respectively. The wide spacing of the contours along the y=x direction is a direct consequence of the positive correlation between the two samples. Qualitatively, this tells that the samples at adjacent transitions are more likely to cause a shift than worst case modulation. As correlation increases, the skewing of the contours will follow suit.

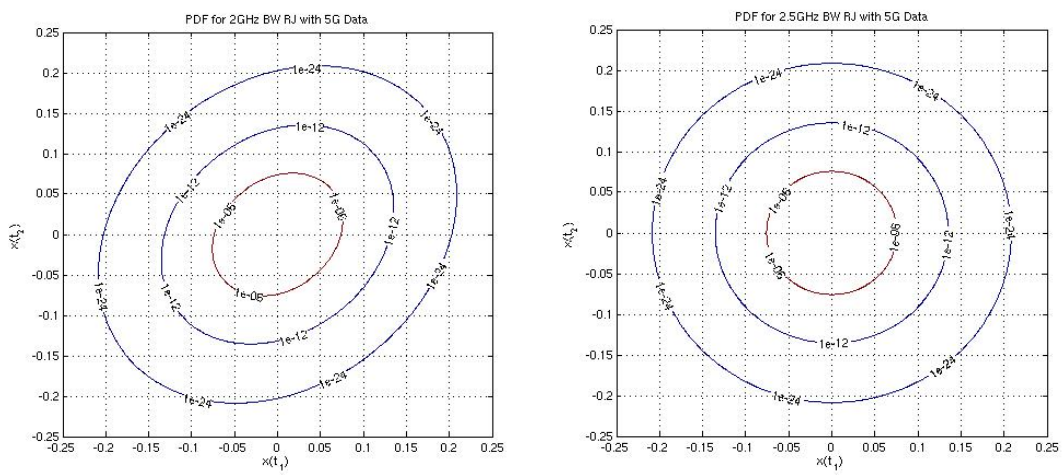

Figure 5: Joint probability contour plots, correlated (left) and uncorrelated (right)

In applications where the variable of interest is from a continuous sample space, the PDF is integrated from + to - ∞, resulting in a CDF. BER curves and CDF plots are common graphical representations of how likely a value will be seen either above or below a point. Integration results in yet another check to ensure the joint PDF description is accurate. Integration over the entire space, ((-∞,∞), (-∞,∞)), must result in a likelihood of one, since an event occurs.

Dependence on previous values, or correlation, limits the magnitude of change over a period of time. The relation between finite frequency content and finite change during a time interval is easily validated via the relationship between correlation and the signal's spectrum. The autocorrelation is simply the inverse Fourier transformation of the spectrum, from the Wiener-Khinchin theorem (JOHNS & MARTIN).

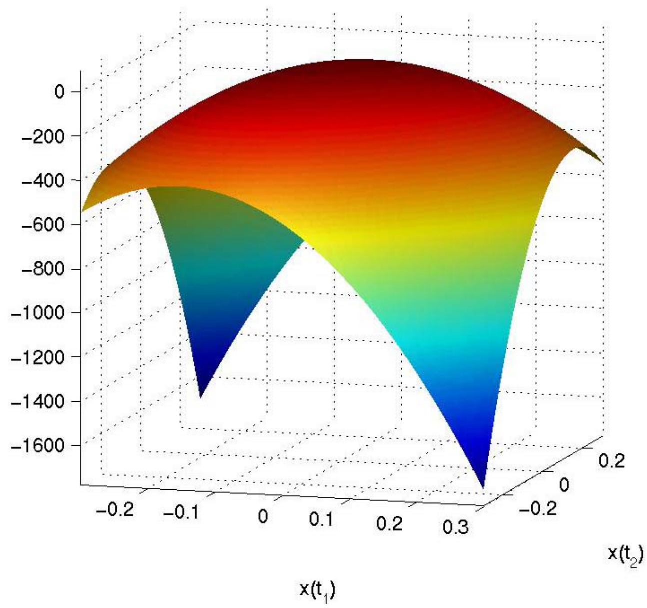

Figure 6: Joint probability distribution

3.2. CORRELATION

Correlation of RJ reduces the highest frequency component on the received signal. This reduces the phase modulation and helps with receiver design by limiting the highest frequency that must be detected to meet a BER. Two approaches are used to confirm this. The first is an analytical derivation of what is mathematically expected, and the second uses Matlab simulations to produce a band-limited phase noise vector and verify the calculated probabilities and pulse narrowing.

The PDF of a Gaussian joint distribution can be extended to the issue of correlation in random phase noise. The correlation coefficient is calculated using spectral information. For this example, band limiting can be viewed as a brick wall low pass filter resulting in an autocorrelation that is a Sinc. The time space between samples is the only remaining information needed to calculate the correlation coefficient. For now, the sampling instances are at t_1 and t_2 and $\tau = t_2 - t_1$. Since the RJ is wide-sense stationary, (COUCH)

Error! Objects cannot be created from editing field codes. (9)

$$\begin{aligned} \mathrm{R}(t_1, t_2) &= \mathrm{R}(\tau) \\ \mathrm{R}(t_1, t_1) &= \mathrm{R}(t_2, t_2) \end{aligned} \tag{10}$$

and the expected value for x is zero, so the equation results in

$$\begin{aligned} \rho &= \frac{\mathrm{R}(\tau)}{\sqrt{[\mathrm{R}(t_1, t_1)][\mathrm{R}(t_2, t_2)]}} \\ &= \frac{\mathrm{R}(\tau)}{\mathrm{R}(t_1, t_1)} \end{aligned} \tag{11}$$

The joint density function for these two sampling points is now used to calculate the distribution for the second sampling instance given the first. The PDF space (Figure 5) is integrated for a fixed width symbol, decreasing towards zero. A fixed width is represented by $y=x-\beta$, integrating x from $[-\infty, +\infty]$. This area represents the probability of all cases where the modulation will be less then the number defined by the value β.

A numerical integration was performed, decreasing the value of β until the desired BER was reached. The result is the minimum pulse width expected during BER=1e-12 operation. If the receiver attenuates this frequency too much, an error will occur.

3.3. SYMBOL MODULATION – ANALYTICAL CALCULATION

The calculated PDF space is numerically integrated according to the previous constant closure bound. The resultant curve illustrates the expected symbol modulation due to RJ. Two cases are used, one for uncorrelated RJ and another for correlated RJ, both relative to the symbol rate.

The bandwidths chosen will be appreciated later, 2GHz and 2.5GHz. The correlation coefficient was calculated for a data rate of 5Gbaud and resulted in 0.2339 and 0, respectively.

$$\begin{aligned} \rho &= \frac{\mathrm{R}(\tau)}{\mathrm{R}(t_1, t_1)} \\ &= \frac{\dfrac{2W \sin(2\pi W \cdot t)}{2\pi W \cdot t}}{\dfrac{2W \sin(2\pi W \cdot 0)}{2\pi W \cdot 0}} = \frac{\sin\left(2\pi 2.5\times10^9 \cdot \tau\right)}{2\pi 2.5\times10^9 \cdot \tau} = \frac{\sin\left(2\pi 2.5\times10^9 \cdot \dfrac{0.8}{2.5\times10^9}\right)}{2\pi 2.5\times10^9 \cdot \dfrac{0.8}{2.5\times10^9}} \\ &= 0.2339 \end{aligned} \tag{12}$$

The two curves in Figure 7 illustrate the expected modulation for 0.3UIpp RJ at a BER of 1e-12.

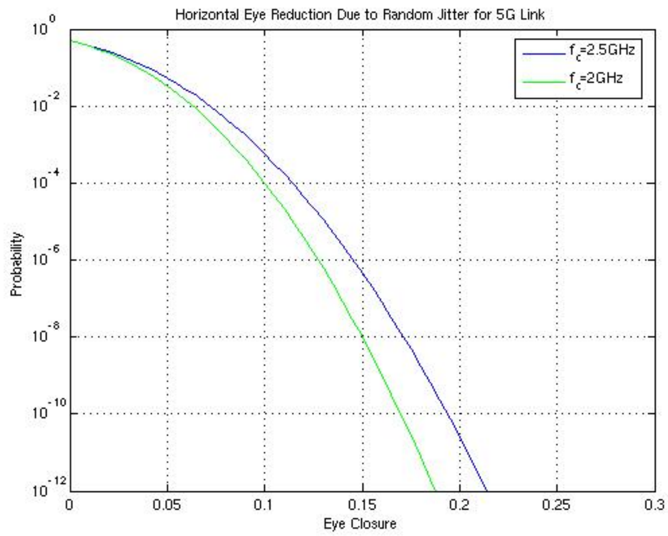

Figure 7: Calculated Eye Modulation Due to RJ

The correlated RJ was found to modulate the signal by 38% less than its peak-to-peak value, while uncorrelated was approximately 27% less than the peak-to-peak for the 1e-12 rate of occurrence.

3.4. SYMBOL MODULATION – SIMULATION

In order to validate these findings, a simulation was performed in Matlab. Multiple Gaussian noise vectors were generated with different seeds. These were then band limited with a high order linear filter to approximate the band limiting, at two different frequencies. The filtered vectors were scaled to have the same power. Measurements were made on the resultant vectors, at 1 UI intervals. The differences between offset values were calculated, binned, and summed to yield the probabilities for each range. The PDF was cumulatively summed from +∞ to zero, and the resultant probability or BER is plotted in Figure 8. You will notice very similar results to the analytical calculation. The differences seen can be attributed to the binning used in the Matlab simulation, and extrapolation of the data.

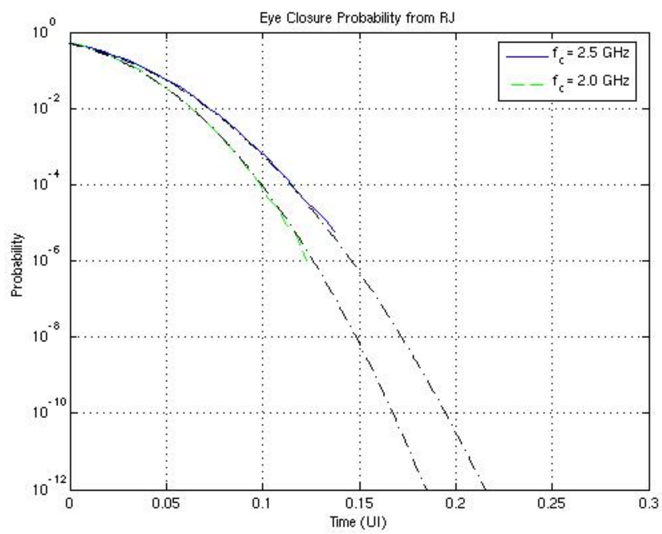

Figure 8: Simulated Eye Modulation Due to RJ

The results seen here are approximately 38% and 28% reduction in modulation from the peak-to-peak numbers, for the 2.5GHz and 2.0GHz bandwidths, respectively. These are very close to those seen in the analytical section.

3.5. SAMPLING

The receive eye template illustrates the expected eye opening as seen at the receiver input. An example is shown in Figure 9. The eye is a region where no signal crossings will occur, making the center ideal for sampling. Errors are minimized at this location. Two primary pieces of information are contained in the eye: the time interval over which a valid sample can occur and the minimum amplitude it will have. Minimum and maximum rise and fall times, respectively, can be computed.

3.5.1. Jitter in Receive Clock

The actual sampling location is controlled by the reference crystal, PLL, and any offset tracking circuitry. The actual sampling process can be visualized as dual windows, shown in Figure 9. The locations where the receive data transitions occur is described by the crossing window. Sampling must take place during the time that remains, the receive eye. A second window surrounds the ideal sampling point. It is within this window that the actual sampling will occur. This sampling window is determined by the jitter from internal components, such as the phase noise in the crystal, clock recovery and synchronization, as well as the jitter in the received signal. In order for negligible effects due to the sampling jitter, the receive eye must be wider than the sampling window.

There is a relation between sampling jitter and receive jitter due to the operation of the clock recovery loop. These relationships are highly implementation dependent and will not be discussed here.

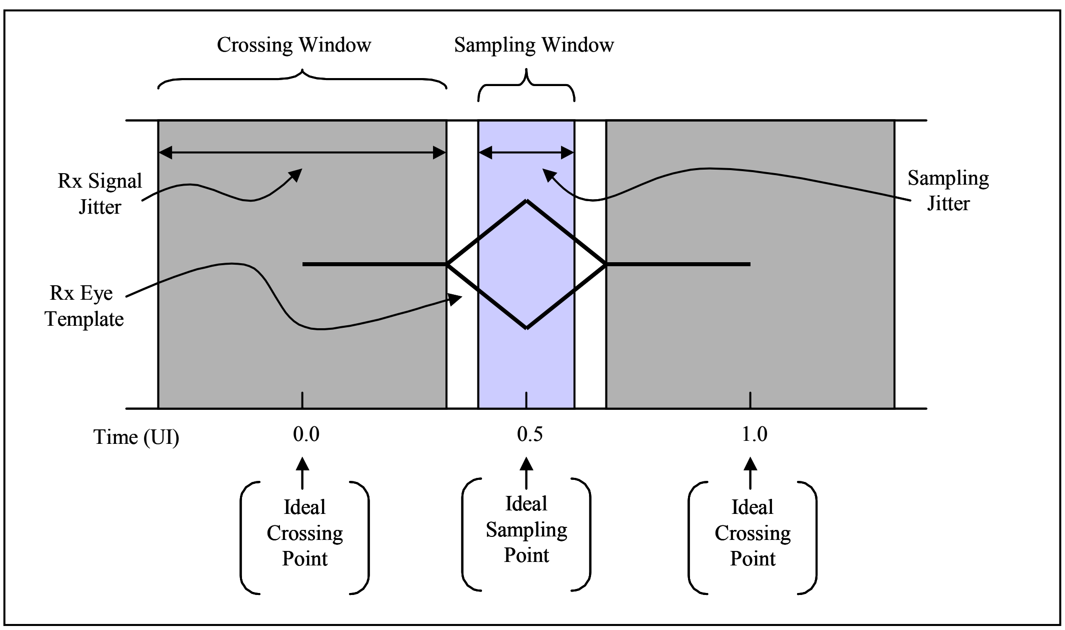

Figure 9: Sampling and Crossing Windows at Receiver

3.5.2. Sampling

The sampling window has another constraint. The received data should remain above a threshold for a minimum amount of time in order to latch the value. Even if the sampling process starts with valid data on the line, the correct value will not be stored if it cannot be latched.

Jitter present on the sampling clock can be attributed to a variety of sources. Both the reference crystal and jitter on the input signal have already been mentioned. Other sources are power supply noise, duty cycle distortion, and other implementation dependent sources.

3.6. TOTAL JITTER RESPONSE

A simplified model for the DJ treats it as entirely ISI with equal shift probabilities. This is taken from OIF and MJSQ, using the Dual Dirac Model for DJ which is an impulse at +/- DJ/2 with magnitude 0.5. Both RJ and DJ are specified at the receiver input, so these effects must be combined by convolving their PDFs.

One type of plot to visualize the relationship between error rates and eye diagrams is known as a bathtub curve (Figure 10). This illustrates the probability of translating the crossing point various distances over one UI. Jitter values for this diagram are 0.3UI RJpp and 0.4UI DJ. The error rate of 1e-12 occurs at an eye width of 0.3UI. The deceiving part here is that all errors are attributed to violating the eye template, implying that the receiver must be able to receive a pulse the width of the eye.

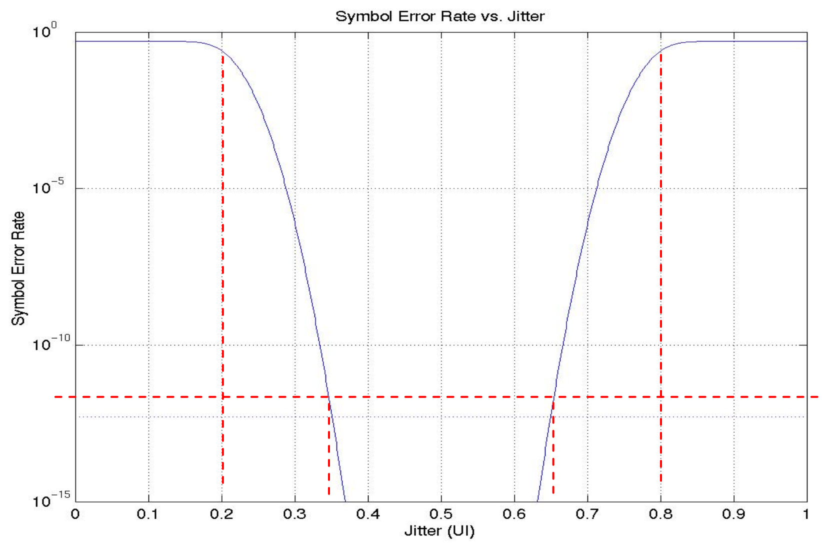

Figure 10: Bathtub Curve for 0.4UI DJ, 0.3UI RJ, BER=1e-12

3.6.1. Design Tradeoffs

The exact concept of what constitutes an error is easy to understand, not detecting a symbol correctly. The end goal for a transceiver is simply to meet a particular error rate. Specifying noise parameters that represent the intended error rate is not as straightforward. The way an error is seen in terms of theoretical analysis must be described in more detail.

Eye diagram violations are a normal first thought. Any symbols that violate the eye will not be received properly, due to shifting, and therefore will result in an error. This is true for one condition. However, there is an added dimension based on the eye width. The combined DJ and RJ, or total jitter (TJ), will determine the probability of actually violating the eye. The likelihood of violating both sides of the eye at the same time, however, is negligibly small. In other words, the receiver will never see symbol durations that short while remaining error free.

Errors occur when the symbols are either too high frequency or a transition has shifted too far in time. Based on knowing the jitter on the received signal and the receiver bandwidth, the BER can be determined. Conversely, the receiver's bandwidth can be determined based on the BER, jitter, and the sampling window.

Errors will be described in terms of the two failure modes. Transition shifting will be referred to as eye template violations. These are the edge shifts of the received signal that cause an error. Modulation errors, on the other hand, occur when the symbol is too high frequency for the receiver to detect it.

Even if the received signal never violates the sampling window, some symbols may be of sufficiently high frequency that the receiver cannot detect them properly. This source of error must be accounted for. Perfect performance in respect to translations allows for error rates up to the BER to be made due to symbol modulation alone.

However, if the shift tolerance of the receiver is not perfect, and it is not, the receiver bandwidth must be set so errors due to shifting are accommodated. The key is having an error rate after combining both sources that is no more than the BER specified.

The correct distribution is determined by the receiver design. Performance tradeoffs can be made to comply with the overall error rate that must be met. The equations that must be satisfied to meet the BER specs are:

$$BER = P(\text{BW violation}) + P(\text{shift violation})$$

$$P(\text{Modulation Error}) = P(x_1, x_1) = P(x_1)^2$$

$$P(\text{shift violation}) = P(x_2) + P(-x_2) = P(x_2)P(-x_2) = 2P(x_2) - P(x_2)^2 \cong 2P(x_2)$$

Modulation Error			Translation Error			Minimum Symbol Width	
% Total Errors	$P(x1)^2$	P(x1)	% Total Errors	P(x2)	P(x2,-x2)	UI	GHz
100	10^{-12}	10^{-6}	0	0	0	0.7972	3.136
1	10^{-14}	10^{-7}	99	$4.95*10^{-13}$	$2.45*10^{-25}$	0.7782	3.213
.1	10^{-15}	$3.16*10^{-8}$	99.9	$4.995*10^{-13}$	$2.495*10e^{-25}$	0.7694	3.249
0	0	0	100	$5*10^{-13}$	$2.5*10^{-25}$	0.70	3.60

Table 2: Eye closure for various error distributions and uncorrelated RJ

Table 2 lists the trade-offs between receive bandwidth and sampling performance. It shows that a slight improvement in sampling window can have a large impact on the maximum frequency signal for a BER.

Improving the sampling performance slightly can widen the minimum pulse, easing design. Improvement in sampling performance can be accomplished by a variety of tradeoffs. Some examples are a reference crystal with less phase noise, faster acquisition time, a better package, etc.

4. APPLICATIONS

The analysis of RJ conducted in this paper has many important applications in industry. They cover the gamete of design, starting with standards development, moving through simulation and verification, and ending with hardware testing.

4.1. SIMULATION

Verification is performed over different conditions to verify system performance. One method is simulating the receiver using a Gaussian source for phase noise, and running for at least 10 errors, or 10/(BER*SymbolRate) to verify the BER is met. However, a receiver simulation using R/RC extracted schematics takes on the order of one day per microsecond. Simulation using pre-layout schematics takes on the order of an hour per microsecond. So, testing BER compliance by this method for the receiver only would take about 90 days, which is not realistic. In order to test the blocks, worst-case inputs are desirable.

For jitter, RJ can be split into two deterministic components. First, the symbol modulation of RJ should be accounted for. This can be done by a variety of ways. One method is applying the highest frequency signal to the receiver to check the attenuation. Another method is applying a uniform random variable with a bound of the maximum expected phase modulation.

Secondly, the symbol translation of RJ should be modeled. This can be done through the use of a data correlated shift vector. A SJ term could also be used, but would take additional time. The SJ frequency should be sufficiently low such that it is not tracked out, nor does it perform pulse width modulation.

The maximum symbol modulation should be removed from the total RJ term to determine the translation component. This simulation is more pessimistic than will necessarily be encountered, but it is designed to test the worst-case condition that the receiver must tolerate error-free.

4.2. DESIGN

Engineers need specific metrics to design to. If those do not exist, odds are that the final product will far exceed performance, cost, and power consumption actually required. Regardless if the RJ is correlated or not, the maximum required frequency can be calculated. It can then be used for the simulations previously described, as well as the bandwidth required to design the front-end.

For example, a receiver might be required to detect a 2.0 GHz (calculated maximum frequency) signal that has minimum amplitude of 175mVpp. If the minimum expected amplitude at the detection circuit is 350mVpp, the receiver's 3dB frequency must be greater than or equal to 2.0GHz.

Design constraints can be traded off based on the earlier analysis of modulation vs. translation errors. If one metric proves difficult to achieve, it can be relaxed while the other is improved.

4.3. TESTING

Physical verification of a design is crucial. The products must be both tested properly, as well as have the proper tests specified to be interoperable. The knowledge of RJ's spectral relationship to maximum received frequency is important when choosing equipment as well as writing the specification.

For example, quite a few verification tests make use of a random noise generator. One such device is the NoiseCom PNG7112, which is their highest frequency generator, emitting a 10MHz-2GHz AWGN signal. However, when testing a 5G SERDES with data rates up to 6.125Gbaud, the edges will be correlated. The curves presented earlier for RJ correlation are representative of the 2GHz BW relationship to the best case 2.5GHz 5Gbaud BW. Even if this device is used in the lab, the results would not match those for an uncorrelated analysis. The correlation can be taken into account for a sanity check of measured results.

5. CONCLUSIONS

The general methodologies discussed for jitter specification are common to many standards, even though no specific serial interface specifications were analyzed during this paper. As these interfaces are used on a broader scale and in faster processes, the margin between success and failure is becoming ever narrower.

The spectrum of signals acting on data is very important for accurately quantifying its characteristics at the input. The calculated results for correlation of the random jitter are shown to be very similar to those seen in simulation. This can be extended to other spectral densities, not just a white band limited case.

If a receiver is designed to the minimum eye frequency, it will result in very high and very unnecessary performance. Also, if the random signal is not in fact white, but falls off at the upper frequencies, the correlation will be even greater at the input.

Various levels of detail are needed depending on the system. For an electrical conductor with little RJ, this detailed analysis might not be needed. In a system with large quantities of RJ, particularly an optical channel, the analysis yields some enlightening pieces of information for proper budgeting and design.

In the end, tradeoffs can be made in the design to relieve pressure on difficult design challenges, while exploiting any easy improvements. When the design is complete and parts come back, the only thing that matters is it meets the specifications.

Accurate simulations are key to this success. Failures have become too costly to be common. Mask sets for 90μm are on the order of $1 million. The bounding of any random effects is key to testing worst-case scenarios and preventing failures. Accurate specification and then testing will both ensure design success as well as allow smaller margins to be used.

6. REFERENCES

Common Electrical I/O (CEI) – Electrical and Jitter Interoperability Agreements for 6G+ bps and 11G+ bps I/O. OIF2003.104.09, Optical and Internetworking Forum, 2004.

Couch II, Leon, *Digital and Analog Communication Systems.* Upper Saddle River, New Jersey: Prentice Hall, 1997.

Fibre Channel – Methodologies for Jitter and Signal Quality Specification – MJSQ. T11.2 / Project 1316-DT/Rev 5.0, February 21, 2002.

HFAN-4.0.3: Jitter in Digital Communication Systems. Maxim IC, 2001.

HFAN-4.0.4: Jitter in Digital Communication Systems. Maxim IC, 2002.

S. Huss and J. Bennett, "An efficient model for twisted-pair cables with discontinuities and stubs for discrete time simulations," *The 2001 IEEE International Symposium on Circuits and Systems*, pp. 254-257 Vol. 4, May 2001.

S. Huss, "A Mathematical and Lumped-Element Model for Multiple Cascaded Lossy Transmission Lines with Arbitrary Impedances and Discontinuities," *The 1995 IEEE International Symposium on Circuits and Systems*, pp. 1844-1847 Vol. 3, 1995.

IEEE Draft P802.3ak/D5.3. New York, New York: IEEE, 2003.

Jitter Fundamentals. Wavecrest Corporation, SMPB-00019 Rev. 1.

D. Johns and K. Martin, *Analog Integrated Circuit Design.* New York: John Wiley & Sons, Inc., 1997.

A. Papoulis and S. Pillai, *Probability, Random Variables, and Stochastic Processes*. McGraw-Hill, 2002.

H. Stark & J. Woods, *Probability, Random Processes, and Estimation Theory for Engineers*. Upper Saddle River, NJ: Prentice Hall, 1994.